

## Trapping of thermal positrons at metal surfaces

Y. Kong and K. G. Lynn

*Department of Physics, Brookhaven National Laboratory, Upton, New York 11973*

(Received 23 May 1990; revised manuscript received 4 June 1991)

The interaction of positrons with a surface potential is considered as a two-step process, upon which the time-dependent positron trapping into the surface potential is evaluated. The reflection of positrons at the surface potential is seen to be larger than previously calculated. This suggests that the interaction of positrons with a surface is a many-encounter process.

### I. INTRODUCTION

With the advent of variable-energy positron beams, it has become possible to study solid surfaces and interfaces with positron techniques.<sup>1</sup> When positrons with keV incident energy are implanted in solids, a majority of them become thermalized with the lattice and diffuse back to the surface as thermal positrons. In interacting with the surface potential, positrons may become trapped by their own image potential and form positron surface states. They may also escape the surface either by picking up electrons to form positroniums (Ps), or may be reemitted as free positrons on negative-work-function surfaces. Considerable theoretical and experimental work has been carried out in order to understand these surface processes. A typical model approach includes treating these possibilities as competing rate processes,<sup>2,3</sup> i.e., the Ps formation rate is  $\nu_{Ps}$ , positron reemission rate is  $\nu_{e^+}$ , surface trapping rate is  $\nu_s$ , and the desorbed fraction of positrons from the surface trapped state via the Ps channel is  $f_d$ . The branching ratios into each of these channels are then calculated as follows:

$$\begin{aligned} \text{total rate } \nu &= \nu_{e^+} + \nu_{Ps} + \nu_s, \\ \text{positron reemission branching ratio } &\nu_{e^+}/\nu, \\ \text{Ps reemission branching ratio } &(\nu_{Ps} + f_d \nu_s)/\nu, \\ \text{surface trapping branching ratio } &(1 - f_d)\nu_s/\nu. \end{aligned} \quad (1)$$

Specifically, the surface trapping rate  $\nu_s$  is calculated using the Fermi golden rule, where the wave functions for both the final localized and initial delocalized positrons are obtained from solving the stationary Schrödinger equations.<sup>4,5</sup>

The branching ratios evaluated from Eq. (1) provided the basis for much of the previous theoretical and experimental work. It is, however, inappropriate because of the following considerations. First of all, positron trapping at a surface potential is a dynamical process, and should be treated on a time-dependent basis. This time dependence becomes more critical when positron trapping is accompanied by other processes such as elastic scattering.<sup>3</sup> Elastic reflection from the surface potential approaches unity for thermal positrons at decreasing tem-

peratures, and there exists the question of whether positron trapping still occurs under such circumstances (note that the stationary Schrödinger equation solution gives a zero delocalized wave function beyond the surface potential well; in other words, the overlapping of the delocalized and localized wave functions approaches zero). If the time-dependent nature of the problem is included, the possible effects of the positron being scattered within the potential well and the corresponding time scale has to be considered to account for positron trapping.

The branching ratios defined in (1) implicitly assume that the different surface processes are competing one-step processes. It will not be proper to apply the theoretically calculated rates to Eq. (1) without justification of the underlying physical model. For example, the procedure used in Ref. 3 distinguishes the time sequence of positron trapping from positron reemission and Ps formation, which would not agree with Eq. (1). A two-step process is assumed there, with the positron being transmitted through the surface potential and experiencing reflection or trapping first, and subsequently the transmitted positrons will undergo the competing processes of escaping as Ps or  $e^+$ . It is obvious that the one-step competing surface trapping rate previously calculated cannot be used in Eq. (1) with this two-step model to obtain the trapping branching ratio.

In an effort to examine the qualitative features when the time dependence is introduced, we attempt to follow the two-step model and calculate the positron trapping at the surface. The temperature, as well as the sign of the work-function effects on the trapping, is evaluated. The theoretical basis used in this calculation is described in Sec. II, with the results and discussions given in Sec. III.

### II. THEORY

Positron trapping at a surface potential is a localized time-dependent perturbation problem. Trapping occurs only when the delocalized positron wave function is close to the surface. The situation resembles that of an ion Auger neutralization process.<sup>6</sup> Suppose at time  $t$  the trapping rate is  $\Gamma(t)$ . The fraction that survives the inelastic trapping will then be

$$P = \exp \left[ - \int_{-\infty}^{\infty} \Gamma(t) dt \right] \quad (2)$$

or the trapped fraction is

$$F_s = 1 - P. \quad (3)$$

For ion neutralization, the trajectory approximation appropriate for ions at certain energies is assumed. A spatially dependent transition rate  $\Gamma(z)$  (usually of exponential form) is then used to solve for the neutralized fraction. For positrons with thermal energies, however, it is more proper to start from the Schrödinger equation, so that the quantum-mechanical nature of positron propagation is considered, and one does not have to assume any form for the transition rate  $\Gamma(t)$ .

In this paper, the time-dependent trapping rate  $\Gamma(t)$  will be evaluated by following the propagation of the delocalized positron wave function and its scattering from the surface potential. With the wave functions obtained, we can evaluate the transition matrix for positron trapping into the surface state. Fermi's golden rule is then applied to yield the time-dependent transition rate, and thus we may determine the trapped fraction from (3). Similar formulation is also used in dealing with the Auger neutralization problem as discussed in Ref. 6.

The surface potential is modeled as a square well as shown in Fig. 1. The discreteness of the lattice, the inhomogeneity of the electron gas, and the long-range character of the image potential, etc., will be neglected here since our main concern is the qualitative nature of a two-step process. The same square potential-well model has been used in many other circumstances<sup>7</sup> for calculations of positron reemission or trapping at surfaces.

The trapped positron wave function and corresponding binding energy are easily solved for such a potential well from the stationary Schrödinger equation. The evaluation of the time-dependent delocalized wave function is based on the Schrödinger equation

$$-\frac{\hbar^2}{2m} \frac{\partial^2 \Psi(z,t)}{\partial z^2} + V(z)\Psi(z,t) = i\hbar \frac{\partial \Psi(z,t)}{\partial t}. \quad (4)$$

The numerical solution of Schrödinger's Eq. (4) needs to preserve the unitarity of the Hermitian operator<sup>8</sup> which is done in our case by carrying the time difference as

$$\left[1 + \frac{1}{2}i \frac{\delta H}{\hbar}\right] \psi_j^{n+1} = \left[1 - \frac{1}{2}i \frac{\delta H}{\hbar}\right] \psi_j^n. \quad (5)$$

The numerical difference equation corresponding to Eq. (4) is both stable and unitary, and it can be solved to obtain at each instant the delocalized free-positron wave function.

$$\psi(z,0) = \frac{1}{(\sigma_0 \sqrt{\pi})^{1/2}} \exp(ik_0 z) \exp\left[-\frac{(z-z_0)^2}{2\sigma_0^2}\right]. \quad (6)$$

A Gaussian wave packet Eq. (6) is assumed for the initial wave function of the incident thermal positron. The momentum spread of the wave packet is associated with the thermal broadening, as is the spatial extent  $\sigma_0$  ( $\sim 60 \text{ \AA} \sqrt{300/T}$ ). This spatial extent is far larger than the width of the potential well ( $\sim 2 \text{ \AA}$ ), which makes the quantum-mechanical calculation more desirable. The centroid of momentum  $k_0$  in this calculation is taken to

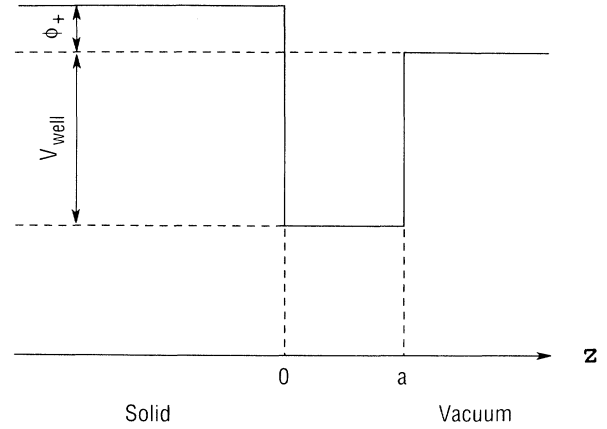


FIG. 1. Schematic representation of the positron surface potential well with a negative positron work function.

correspond to the thermal energy of positrons, and  $z_0$  is the starting position of the wave packet.

If  $\mathbf{k}$  and  $\mathbf{p}$  are the initial electron and positron momenta and  $\mathbf{q}$  is the momentum transfer, then the transition rate from the delocalized state to the bound state is calculated with Fermi's golden rule<sup>5</sup> as

$$\Gamma = \frac{2\pi}{\hbar} \sum_{\mathbf{p}} \sum_{\mathbf{q}} |M(\mathbf{p}, \mathbf{q})|^2 f_{\mathbf{k}} (1 - f_{\mathbf{k}+\mathbf{q}}) \delta(\varepsilon_i - \varepsilon_f), \quad (7)$$

where  $f_{\mathbf{k}}$  is the step function  $\Theta(k_F - k)$ ,  $k_F$  is the Fermi momentum, and

$$\varepsilon_i = \frac{\hbar^2 \mathbf{k}^2}{2m_-} + \frac{\hbar^2 \mathbf{p}^2}{2m_+},$$

$$\varepsilon_f = e\phi_+ - \varepsilon_b + \frac{\hbar^2 (\mathbf{k} + \mathbf{q})^2}{2m_-}.$$

Here,  $\varepsilon_b$  is the positron binding energy at the image potential,  $\phi_+$  is a positron surface work function and  $m_+$  and  $m_-$  are the positron and electron effective mass in solids.

The electron wave function as well as the transverse components of the positron wave function are represented by plane waves with perpendicular momentum transfer  $q_z$ , and the matrix element is evaluated as

$$M(\mathbf{p}, \mathbf{q}) = \frac{v(\mathbf{q})}{L^3} \int dz e^{iq_z z} u_i(z) u_f(z), \quad (8)$$

where the initial delocalized positron wave function  $u_i(z)$  is obtained from Eq. (4), and  $u_f(z)$  is the normalized positron bound state.  $v(\mathbf{q})$  is the Fourier transform of the screened Coulomb interaction, the screening constant will be assumed to be a fraction of the bulk Thomas-Fermi screening constant,<sup>7</sup> and  $L$  is the normalization length.

The electron-hole mediated trapping rate for a surface of positron work function  $\phi_+$  is from Eqs. (7) and (8),

$$\Gamma = \frac{mk_F}{8\pi^4\hbar^3} \int d\mathbf{p} \int dq q |\nu(\mathbf{q})|^2 \chi \left( \frac{q}{k_F}, \frac{\frac{1}{2}p^2 + m\varepsilon_b - me\phi_+}{\hbar^2 k_F^2} \right) \int dz \int dz' u_i^*(z) u_f(z) u_i(z') u_f^*(z') \frac{\sin(z-z')q}{z-z'}. \quad (9)$$

Here,

$$\chi(x, y) = \begin{cases} \frac{\pi}{x} \left[ 1 - \left( \frac{y}{x} - \frac{1}{2}x \right)^2 \right], & x + \frac{1}{2}x^2 \geq y \geq |x - \frac{1}{2}x^2| \\ \frac{2\pi}{x} y & \text{for } 0 \leq y \leq x - \frac{1}{2}x^2 \text{ and } x < 2 \\ 0 & \text{otherwise.} \end{cases}$$

We should note that though the delocalized wave function changes significantly spatially as time proceeds, the momentum distribution does not change until the incident wave packet in the configuration space enters the range of the surface potential.<sup>9</sup> When the incident wave packet does get into the potential well, the magnitude of the centroid of the momentum distribution will change about  $k_0$  only because of the elasticity of the scattering process. An approximation in Eq. (9) is made by neglecting the integration over initial positron momentum spread and evaluating the trapping rate at the centroid of the momentum,  $k_0$ , only. This is acceptable considering other simplifications in the problem.

The trapping rate is calculated for different temperatures and work-function surfaces. The transmitted elastic fraction can be obtained by examining the transmission coefficient from our calculation, from which an estimate of the surface trapped branching ratio is obtained.

### III. RESULTS AND DISCUSSIONS

The time-dependent trapping rate for an initial Gaussian wave packet is evaluated. Figure 2 shows the time-dependent trapping rate at 100, 200, and 300 K for (a) a negative work-function surface and (b) a positive work-function surface. The parameters of the surface potential are listed in Table I. It is noted here that the temperature dependence of certain parameters is not considered, e.g., the positron work function, thermal Ps desorption, etc. Positron annihilation and Ps formation during the trapping process are not considered.

For the negative work-function surface [Fig. 2(a)], it is seen that at low temperatures, the maximum amplitude of positron trapping is reduced from that of high temperatures. This is mainly associated with the stronger reflection at the surface potential well at reduced temperatures. The reflection occurs dominantly at the inner side of the surface potential ( $z=0$  in Fig. 1), thus the transition matrix as well as the trapping rate have only one maximum. The same effects can be seen in Fig. 3(a), which shows the time-dependent positron fraction beyond the surface potential ( $z > a$  in Fig. 1) for different temperatures. This quantity approaches the transmission coefficient at longer times. The transmitted fractions at lower temperatures are always reduced owing to reflection, whereas the initial increase of this quantity is

monotonic with time and is associated with the reflection occurring at  $z=0$ .

The positive work-function surface result [Fig. 2(b)] is different from a negative one in several respects. First of all, the absolute amplitude of the trapping rate is reduced relative to the negative work-function surface case. This is because of the strong repulsion that a positron experiences from both the inner step ( $z=0$ ) and the vacuum side of the potential ( $z=a$ ). Second, there exist oscillations in the calculated trapping rate and transmitted fraction [Figs. 2(b) and 3(b)], which are also related to the importance of reflection at  $z=a$  for a positive work-function surface. Since positrons elastically reflected at  $z=a$  may get trapped on their way back into the solid. This quantum-mechanical effect is also observable in the time-dependent transmitted fraction in Fig. 3(b), where some positrons may be temporarily present on the vacuum side ( $z > a$ ) even though they are eventually reflected back into the solid. The same phenomenon is negligibly small for a substantially negative work-function surface, where most of the reflection happens at the solid side of the potential well. It should also be noticed from Fig. 2(b) that the reflected positrons contribution to the trap-

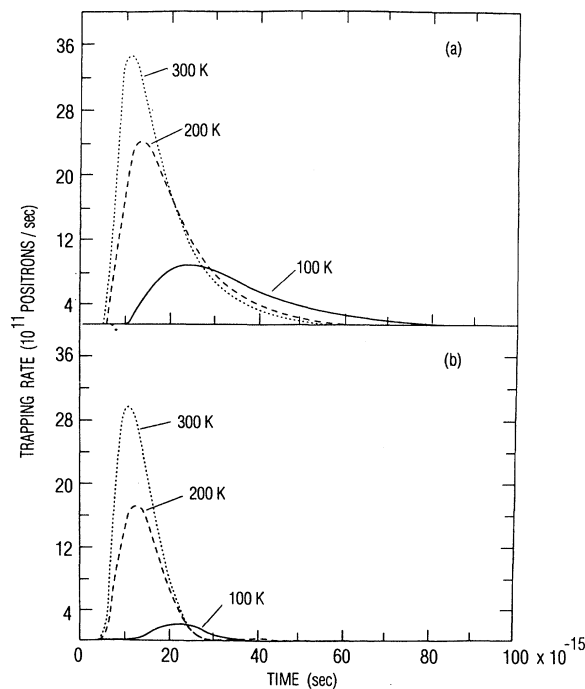


FIG. 2. (a) The time-dependent trapping rate for a negative work-function surface at  $T=100, 200,$  and  $300$  K. (b) The time-dependent trapping rate for a positive work-function surface at  $T=100, 200,$  and  $300$  K.

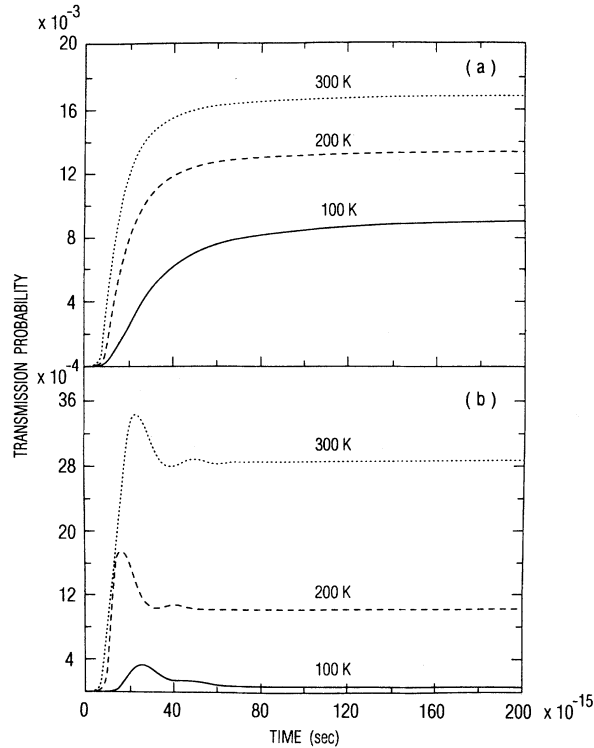


FIG. 3. The time-dependent fraction of positrons present beyond the surface potential in the vacuum side ( $x > a$  in Fig. 1): (a) for a negative work-function surface at  $T=100, 200,$  and  $300$  K; (b) for a positive work-function surface at  $T=100, 200,$  and  $300$  K.

ping rate is very small compared with the initial outgoing positron contribution. Thus the total trapped fraction will still be more dependent on the reflection at  $z=0$ . From this result it may be inferred that the absolute magnitude of trapping will be reduced when the temperature is decreased even for positive work-function surfaces.

The trapped fraction evaluated from the time-dependent trapping rate [Eq. (3)] is shown in Fig. 4. This quantity is related to the positron dwell time (which consists of the time spent by the transmitted and reflected positrons in or near the potential-well region) and the strength of the transition matrix within the dwell time. The temperature dependence here is decided not only by reflection, but also by the time it takes for the positron to travel through the potential well. The positron trapped fraction almost doubles in the discussed temperature

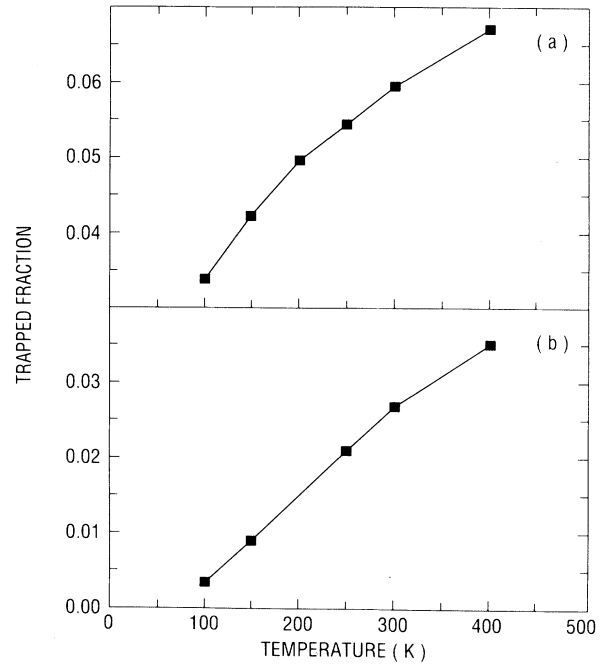


FIG. 4. (a) The temperature dependence of the trapped fraction for a negative work-function surface. (b) The temperature dependence of the trapped fraction for a positive work-function surface.

range. The transmitted fraction also increases at almost the same rate as shown in Fig. 3, therefore the temperature dependence obtained here is predominantly from the reflection by the surface potential. It should be noted that the trapped fraction in Fig. 4 is different from the trapping branching ratio defined in (1), as will be discussed later.

The transmitted fraction obtained from our calculation is found to be less by one order of magnitude than that obtained previously for a negative potential step (see, e.g., Ref. 3), which is

$$\tau = \frac{4k_B T(k_B T - 2\phi_+)}{[k_B T - \phi_+ + \sqrt{k_B T(k_B T - 2\phi_+)}]^2} \quad (10)$$

There, the image potential well was neglected while only the work-function difference was considered, yielding a transmitted fraction of unity order. We argue that this is inappropriate since the quantum-mechanical scattering from the image potential well does play a role even at zero temperature. Consider the extreme case of a zero

TABLE I. Parameters for the surface potential

Surface studied	Well depth (eV)	Well width ( $\text{\AA}$ )	Binding energy (eV)
Positive work function (0.2 eV)	6	1.5	1.69
Negative work function (-0.3 eV)	6	1.5	2.03

work-function surface ( $\phi_+ = 0.0$  in Fig. 1); the transmission probability is predicted to be unity from Eq. (10), but the transmission coefficient for a potential well from solving the exact Schrödinger equation is<sup>10</sup> on the order of  $10^{-2}$  for thermal positrons. Thus the potential-well depth cannot be neglected when estimating the transmitted or reflected fraction. Instead of estimating the transmitted fraction from Eq. (10), it will be more proper to include the effects of the potential "well." The small transmission coefficient gives rise to a trapped fraction of the same magnitude, while the reflected fraction is the dominant part here. Relating to existing experimental evidences,<sup>3</sup> we may infer that positron interaction with the surface is a many-encounter process.<sup>10</sup>

Figure 4 gives the trapped fraction  $F_s$  for an incident Gaussian wave packet; it is different from the branching ratio defined in Eq. (1), which is a relative quantity disregarding the reflected positrons. One can make an estimation of the trapped branching ratio from the transmitted fraction,  $\tau$ , as follows: if the transmitted fraction is taken as  $(1 - F_s)\tau$ , then the trapped branching ratio is approximately

$$F_s / [F_s + (1 - F_s)\tau]. \quad (11)$$

Equation (11) is plotted in Fig. 5 for both positive and negative work-function surfaces at different temperatures. It is seen that the trapping branching ratio changes very little with temperature and the trapping is relatively enhanced for the positive work-function surface. This agrees with previous experimental findings.<sup>3</sup> It is also noted here that Fig. 5 shows only the qualitative temperature behavior of the trapping branching ratio; the quantitative result is dependent on a more precise model as well as on the choice of certain parameters such as the Thomas-Fermi screening constant at the surface.<sup>7</sup>

In conclusion, we have calculated positron trapping at a surface potential from a two-step model. Positron trapping is affected by the surface potential scattering and the dwell time of positrons in or near the well region. The perturbation approach is considered justified here by the smallness of the trapped fraction from our calculation. We also note that the reflected positron fraction is much larger than previously suggested. As to the temperature

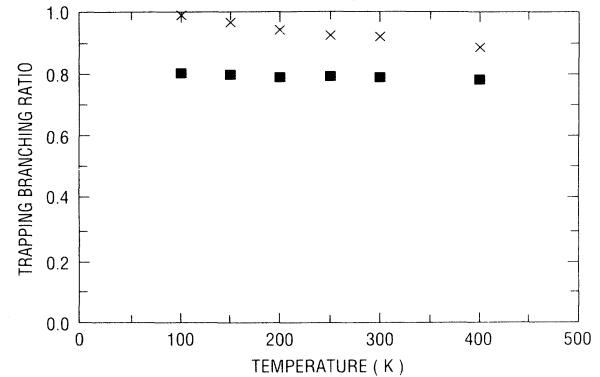


FIG. 5. The relative branching ratio of the trapped positron from a negative positron work-function surface (squares) and from a positive positron work-function surface (crosses).

dependence for electron-hole mediated trapping, the trapped fraction is found to increase with temperature. The relative branching ratio in Fig. 5, however, has a weak temperature dependence in agreement with previous experimental work.<sup>1</sup> In order to fit the present model to the experimental results, the effect of the reflection and other quantitative differences should be further examined. It should also be noted that although this calculation has made some progress from previous calculations, it is nevertheless not perfect in the sense that not only have certain approximations been made, but also the quantitative results, e.g., the relative branching ratio, are subject to the choice of parameters such as the surface Thomas-Fermi screening constant. Improvements of these aspects are planned to be pursued in the future.

#### ACKNOWLEDGMENTS

Dr. J. Throwe is thanked for useful suggestions. Professor R. Nieminen and Dr. J. Davenport are thanked for helpful discussions. Work at Brookhaven National Laboratory was supported by the U.S. Department of Energy, Division of Material Sciences, Contract No. DE-AC02-76CH0001.

<sup>1</sup>P. J. Schultz and K. G. Lynn, *Rev. Mod. Phys.* **60**, 701 (1988).

<sup>2</sup>H. J. Kreuzer, D. N. Lowy, and Z. W. Gortel, *Solid State Commun.* **35**, 781 (1980).

<sup>3</sup>D. T. Britton, P. A. Huttunen, J. Makinen, E. Soininen, and A. Vehanen, *Phys. Rev. Lett.* **62**, 2413 (1989).

<sup>4</sup>R. M. Nieminen and J. Laakkonen, *Appl. Phys.* **20**, 181 (1979).

<sup>5</sup>M. J. Puska and M. Manninen, *J. Phys. F* **17**, 2235 (1987).

<sup>6</sup>H. D. Hagstrum, *Phys. Rev.* **96**, 336 (1964).

<sup>7</sup>D. Nielson, R. M. Nieminen, and J. Szymanski, *Phys. Rev. B* **33**, 1567 (1986).

<sup>8</sup>A. Goldberg, H. M. Schey, and J. L. Schwartz, *Am. J. Phys.* **35**, 177 (1967).

<sup>9</sup>A. Goldberg, H. M. Schey, and J. L. Schwartz, *Am. J. Phys.* **36**, 454, (1968).

<sup>10</sup>Y. Kong and K. G. Lynn (unpublished).